African Journal of Advanced Pure and Applied Sciences (AJAPAS)
Online ISSN: 2957-644X
Volume 3, Issue 3, July-September 2024, Page No: 1-11
Website: *https://aaasjournals.com/index.php/ajapas/index*
معامل التأثير العربي 2023: (1.55) SJIFactor 2023: 5.689 ISI 2022-2023: 0.557

Examination of the Mellitah Oil and Gas Complex's AISI 304 Stainless Steel Transmission Superheated Steam Pipeline: (Corrosion Failure)

Abdulsalam Salama [1*], Mohammed Al-Madani [2], Salah Gnefid [3], Emhemed Madi [4], Abdul-Hamid Ibrahim [5]
[1] Department of Petroleum Engineering, Faculty of Engineering, Al-Zaytoonah- Tarhuna-Libya.
[2] Department of Materials & Corrosion Engineering, Faculty of Engineering, Sebha University, Sebha, Libya.
[3] Department of Mining, Natural Resources Faculty, Al-Jufrah University -Soknah-Libya.
[4,5] Department of Mechanical Engineering, Faculty of Engineering, Al-Zaytoonah- Tarhuna-Libya.

اختبار خط أنبوب نقل البخار المحمص والمصنوع من الفولاذ المقاوم للصدأ: (اختبار التآكل)

عبد السلام حسن سلامة [1*]، محمد الكيلاني المدني [2]، صالح عبد الله قنيفيد [3]، أمحمد محمد مادي [4]، عبد الحميد أبوبكر أبراهيم [5]
[1] قسم هندسة النفط، كلية الهندسة، جامعة الزيتونة، ترهونة، ليبيا
[2] قسم هندسة المواد والتآكل، كلية الهندسة، جامعة سبها، سبها، ليبيا.
[3] قسم التعدين، كلية الموارد الطبيعية، جامعة الجفرة، سوكنة، الجفرة، ليبيا.
[5،4] قسم الهندسة الميكانيكية، كلية الهندسة، جامعة الزيتونة، ترهونة، ليبيا.

[*]Corresponding author: a.salamah@azu.edu.ly

Received: April 21, 2024	Accepted: June 30, 2024	Published: July 04, 2024

Abstract:
Since petrochemical companies frequently employ 304 stainless steel pipes, this study was carried out on the same kind of pipe to examine the early failure of the high-pressure steam coil used in the fuel exhaust unit at Mellitah Industrial Complex. This failure manifested as vapor leaking through the spool's exterior surface fissures, which were evident. The hardness test, X-ray examination, microscopic inspection, visual inspection, and chemical analysis were the most crucial tests carried out to assess the metallurgical failure. The surface of the stainless-steel pipe had pitting erosion, as seen by the microscopic investigation photographs, the presence of this corrosion was confirmed after grinding and smoothing the surface of the sample There is a good explanation why the ingot got damaged. Stress corrosion cracking (SCC) was discovered throughout the interior structure of the stainless-steel pipe, as shown by an X-ray inspection. The presence of the fractures was also visible in the microscopic photographs. By comparing the results of the chemical analysis as well as the hardness test obtained in this research with international specifications, it was found that they conform to them, and this refutes what was stated in the reports of the Mellitah oil and gas complex that the type of corrosion that occurs in the superheated steam transmission pipe is corrosion resulting from thermal fatigue.

Keywords: Stainless Steel, Corrosion, Visual Inspection, X-Ray, Hardness Test.

الملخص
يعتبر أستخدام الفولاذ المقاوم للصدأ شائعاً في المعامل البتروكيميائية. أجريت هذه الدراسة لغرض لتحديد أنواع التآكل التي يتعرض لها هذا النوع من الفولاذ والمستخدم في صناعة أنبوب نقل البخار المحمص في درجات الحرارة العالية في مجمع مليتة للنفط والغاز بليبيا. من خلال الفحص النظري لوحظ وجود تسرب للبخار من خلال شقوق على السطح الخارجي للأنبوب. أهم الفحوصات التي تم أجروها في هذا البحث تشمل: الفحص النظري والفحص المجهري والفحص بالأشعة السينية والتحليل الكيميائي وكذلك أختبار الصلادة. من خلال الفحص المجهري تبين وجود تآكل تنقري وهو سبب وجيه لتلف الأنبوب وحدوث تسرب للبخار، وتم التأكد من وجود هذا التآكل وذلك بعد إجراء عملية تجليخ وتنعيم لسطح العينة. من خلال الفحص بالأشعة السينية تبين وجود نوع أخر من التآكل هو التآكل الأجهادي عبر حبيبات التركيب الداخلي للسبيكة، وقد ظهر هذا أيضا في الصورة المجهرية. بمقارنة نتائج التحليل الكيميائي وكذلك أختبار الصلادة المتحصل عليها في هذا البحث مع

المواصفات العالمية، تبين أنه مطابقة لها، وهذا يفند ما جاء في تقارير مجمع مليتة للنفط والغاز بأن نوع التآكل الذي يحدث في أنبوب نقل البخار المحمص هو تآكل ناتج عن الكلل الحراري.

الكلمات المفتاحية: الفولاذ المقاوم للتآكل، التآكل، الفحص النظري، الأشعة السينية، أختبار الصلادة.

Introduction

An iron alloy that resists corrosion and rusting is called stainless steel. Depending on the element's precise purpose and cost, it may also contain chromium, iron, molybdenum, carbon, nickel, and nitrogen. The reason stainless steel resists corrosion is that it contains 10.5% or more chromium, which creates a passive layer that can shield the material and self-heal when exposed to oxygen [1]. Because of their exceptional resistance to corrosion and degradation in harsh conditions, stainless steels has found extensive application in a wide range of fields. The qualities of the stainless steel that is utilized and the surrounding circumstances affect these attributes. The microstructure, surface condition, and content of alloying elements are attributes of stainless steel that can affect its corrosion resistance [2]. Since austenitic stainless steel type, AISI 304 has better corrosion resistance under typical temperature and condition circumstances, it is widely used in petrochemical, thermal power plants, boiler parts, pressure vessels, etc. But in an oxidizing or dangerous environment, particularly at high temperatures, the alloy's surface is severely damaged, leading to the development of chromium oxide (Cr_2O_3), nickel oxide (NiO), or iron oxide (Fe_2O_3) scales [3]. Temperature, pH, the rate of CO_2 release, and the concentrations of carbonate ions all have a significant impact on the formation of alkaline scales [4].

Corrosion can be defined as the degradation of a material or its characteristics due to external or internal factors interacting with it, or as the harm caused when two or more materials or their constituents come into contact with one another while an auxiliary medium, like heat, moisture, or salts, is present [5]. Many industries, including transportation, infrastructure, industry, and facilities, may be impacted by this natural process. Engineered materials (metals, alloys, polymers, paint, and rubber), covalent and ionic materials, and aggregates (concrete and composite materials) can all be impacted [6]. According to the 2016 "International Measures of Prevention, Application and Economics of Corrosion Technology (IMPACT)" research published by NACE International, the global cost of corrosion is estimated to be around US$2.5 trillion [7].

This study examines the failure analysis of an AISI 304 stabilized stainless steel pipeline in the Millitah oil and gas complex, following years of acceptable operation on steam transfer under high temperatures and pressures. The pipeline is operating under extreme pressure and temperature conditions. These factors resulted in pipeline deterioration that showed up as longitudinal cracks that started on the inside. Studying the causes and effects of stainless steel AISI 304 failure at the Milletah plant's gas incinerator is the primary goal of this project. Next, a variety of tests will be conducted in this regard to look into and document all the factors that contribute to this failure. Ultimately, the findings of this research are essentially examined and contrasted with those of previous studies on stainless steel.

In (2024), Xiaohui Zhang, et, al., in this work, the corrosion behavior of 304 stainless steel (304 SS) in supercritical water (798 K/24 MPa) was examined. Weighing, scanning electron microscopy (SEM), X-ray diffraction (XRD), energy dispersion spectroscopy (EDS), and X-ray photoelectron spectroscopy (XPS) were used to examine the oxidation kinetics, surface morphology, and element diffusion of 304 SS after it had been soaked in supercritical water for 200 hours. Isolated and irregular oxidation deposition is seen on the surface of 304 stainless steel. The oxide layer is found to be a single layer that is primarily made up of spinel that is rich in iron and carbon, with a small quantity of magnetite adhered to its surface. Furthermore, since some pores were discovered on the surface as a result of pitting, the oxidation mechanism was also investigated [8].

In (2022), V. Zatkalíková, et. al., in this study, the corrosion behavior of sensitized AISI 304 stainless steels at 20 ± 3 °C and 50 °C is studied in an acidic 1 M chloride solution (pH = 1.1). In order to determine how the surface condition affects corrosion resistance, the specimens are evaluated both after being sensitized and when they are coated in high-temperature surface oxides, or "heat tinted." Separate corrosion testing, potentiodynamic polarization (PP), and exposure immersion experiments are employed. SEM and optical microscopy (OM) are used to assess the microstructure before and after the immersion test. The findings demonstrated that, even in the absence of high-temperature oxide removal, sensitization considerably conditions corrosion, with high temperatures primarily serving as an accelerator [9].

In (2020), A. Arifin,, et, al., in this study, the failure analysis of a petrochemical plant's AISI304 stainless steel pipeline—which was welded—used to transport CO_2 is presented. Some years of satisfactory operation were followed by the discovery of substantial cracking near the pipeline and valve weld joints. Utilizing optical and fractography, microhardness measures, X-ray fluorescence (XRF), and X-ray diffraction (XRD) tests, the failure research was conducted on welded pipe samples. Defects are found in the heat affected zone (HAZ) region, according to the hardness test results. Analysis of the fractured surface's morphology and macrostructure reveals an intergranular brittle fracture mechanism. Heavy intergranular corrosion, particularly on the outside of the metal surface, is the first sign of an intergranular fault and spreads gradually inside. The secondary carbide peak was identified by XRD data [10].

In (2020), Wei-min Guo, et. al., this study examined the failure analysis of a chemical plant's broken SS304 stainless steel elbow. The elbow lasted for two years and eight months. Two straight pipes were welded to both ends of the elbow. The majority of the crack locations were at the weld joint and the arc, where there was a significant amount of residual tensile stress. The elbow's interior surface was speckled with corrosion pits. The rusting pit bottoms caused cracks to start. Visible branches were emerging from the fissures. energy-dispersive X-ray spectroscopy (EDS) analysis revealed the presence of chloride (Cl) and sulphur (S) elements in corrosion products originating from cracks and corrosion pits. The fracture's transgranular and intergranular brittleness were examined using scanning electron microscopy (SEM) data. Finally, it is determined that stress corrosion causes cracking (SCC) [11].

Material and methods

Case Problem

A 12.7-mm-thick sample of 300-class stainless steel of type H 304 was taken from a spool used in the superheated steam transmission lines in the fuel exhaust equipment. The spool enters the superheater steam horizontally at a pressure of 46 bar and 400 C, with a flow rate of 25801 kg/h. The superheated steam enters the spool vertically in the first quarter, under 70 bar and 131 °C, and exits the spool with superheated steam that is 50 degrees lower than the entry temperature. Figure 1 shows the mechanism of spool working. As illustrated in Figure 2, deep longitudinal cracks appear in this spool, which is coded 584-HL001-51, after the superheated water vapor and boiler feed water spray have mixed for approximately 10 cm.

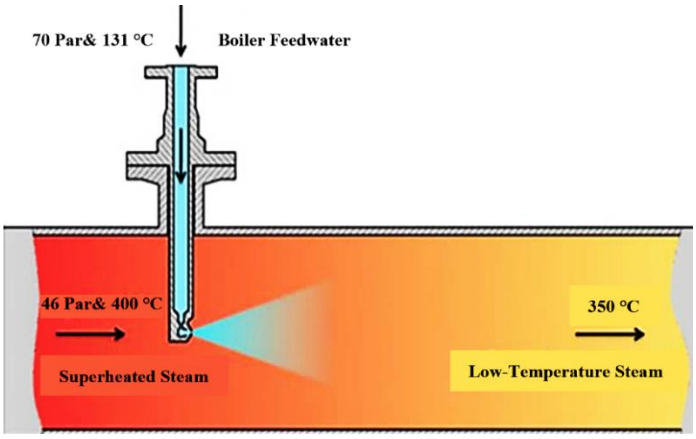

Figure 1: Mechanism of the Spool Working.

Visual Examination (Macro- Fractographic Observation)

One of the most widely used and effective non-destructive testing methods is visual examination. Sufficient lighting of the testing area and the examiner's eyes are necessary for visual examination [12]. In the present research, the experiment was implemented under supervision of engineers of the Advanced Center for Technology - Tripoli.

The sample is situated in the three zones of the thermal incinerator, as seen in Figure 2. This investigation was conducted in the third zone, which is related to steam superheating, while the other two zones are related to gas combustion. In order to do an investigation on damaged equipment, a small sample measuring 15.5 cm in length and 11 cm in width was cut.

Figure 2: The Shape of the Crack in the Spool Before Cutting.

Microscopic Examination (Micro-Fractographic Observation)

The way this method works is that light interacts with the material that makes up the item or sample that is being seen to create images. It is important to refresh our memory about the characteristics of the electromagnetic spectrum. Encompassing wavelengths ranging from thousands of kilometres (km) to a fraction of a nanometre (nm), the electromagnetic spectrum is the range of all electro-magnetic radiation. It starts at low frequencies used for radio and goes beyond very long wavelengths to very high frequency gamma radiation at the short wavelength end of the spectrum [13]. A properly prepared specimen is the only way to observe the microstructure of a material under a light microscope. While this method can, in theory, be used to analyse ceramics and polymers in addition to metallic materials, in fact, some adjustments are required, and caution is advised. The following are the primary procedures in specimen preparation for light microscopy: sectioning, mounting, grinding, polishing, and etching [14]. Figures 3 a and b show the cutting machine and molding device respectively.

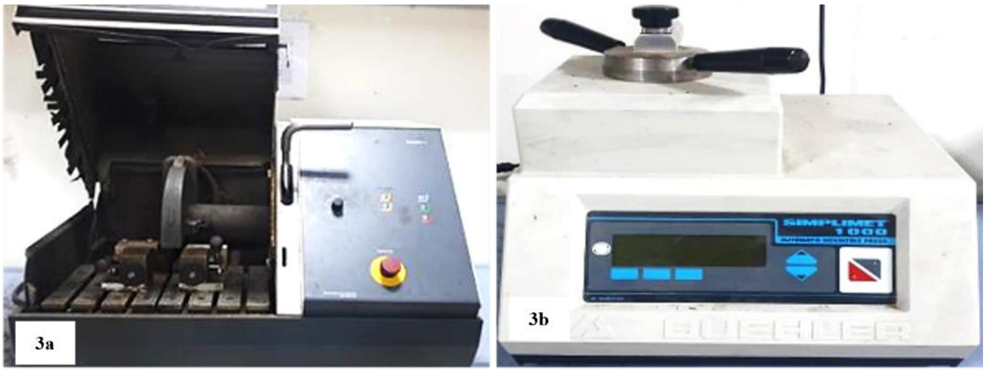

Figures 3a and b: The Cutting Machine and Molding Device Respectively.

Figures 4 a and b show the final appearance of the two subjects, part of the crack area (a), and part of the intact area of the same sample (b).

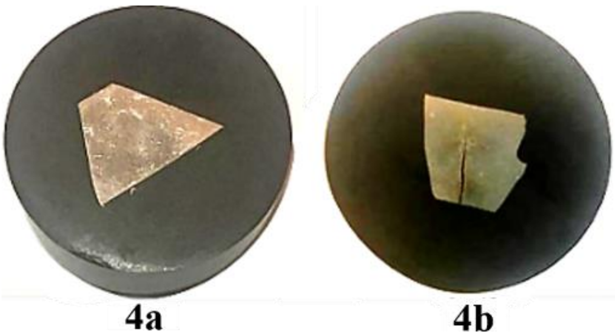

Figures 4a and b: The Samples After Mounted.

The sample must be divided into two portions, a and b, in order to perform this test. The sample's damaged area is shown in image (a), and the sample's undamaged area is shown in image (b). The foundation of this test is based on comparing the structure sample both before and after damage (to identify any changes). It is crucial to stress that the goal of this test is to locate the source and track the break. Essentially, the test approach is based on tracking the crystalline boundaries of the grains. Additionally, each sample (a and b) was inserted into the apparatus and subjected to heat and pressure addition to the plasticizer. To determine the determine the microstructure, crystalline borders, and size of enlarged cracks, an Olympus light microscope, as illustrated in Figure 5, was used.

Figure 5: The Olympus Light Microscope and their Accessories.

X-Ray Fluorescence Analysis

One physical method for quick elemental analysis is X-ray fluorescence (XRF) spectroscopy. It allows the chemical composition to be ascertained for concentrations ranging from ppm to 100%, both in main elements and in traces.

The method of operation involves subjecting a sample to an intense stream of X photons, which causes the sample's constituent elements to emit X-rays. This process is known as X fluorescence. A dispersive system must be present in order to analyse these X-rays. One method does this by using the phenomenon of X-ray diffraction by crystals (Wavelength Dispersion X Fluorescence Spectrometer, WD-XRF), and another method uses the sensitivity of specific sensors to the energy of the photons detected (Energy Dispersion X-Fluorescence Spectrometer, ORC-XRF) [15].

Stainless steel 304 sample's chemical makeup is analysed and compared to standards in this test. Figure 6 illustrates how the sample was made: an electric saw was used to cut a small piece of material, which was then put in a device that was connected to a computer to display the findings. The sample emits an electric spark during combustion, which must be noted.

Figure 6: XRF Analyzer Used in the Present Work.

Radiographic Testing

Radiographic testing is a technique used to find hidden, internal faults in a wide range of materials and combinations. It is also appropriate for thickness measurements and the detection of changes in material composition [16]. In order to perform a radiography test, short-wave X- or gamma radiation must be produced and directed toward an object. To the extent that radiation can flow through an item, it can permeate matter. If this is the case, the radiation can be recorded on a recording medium that is positioned against the object's opposite side.

A variety of digital radiation detectors or industrial X-ray film can be used as the recording medium. The film will be exposed to the radiation that travels through the component, creating a shadow of the component. The amount of radiation that enters the film through the test object will determine how dark or dense the film is [16].

Under the direction of the Libyan Advanced Professional Centre for Welding Technologies, this test was conducted. The following fundamental actions were performed in this test: Utilize the entire sample for the experiment; the imaging film has adhered to the sample's inside using adhesive tape, and the sample with the film was placed under the ANDREX 225 X-ray machine as seen in Figure 7a. After that, the following steps were carried out: the sample was put in developer acid solution as shown in Figure 7b, the sample was put in water basin for 3 minutes, the sample was placed in acid for 4 minutes in order to stabilize the image, the sample replace again in water in purpose of cleaning and get rid of remnants of solutions, Finally, the sample was dried in devices as shown in Figure 7c.

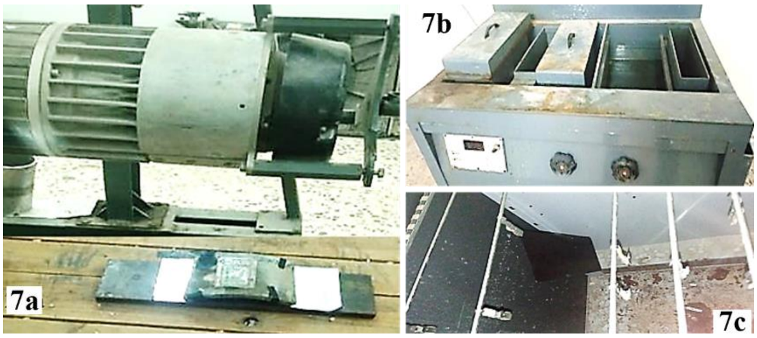

Figures 7a, b and c: Radiographic Testing Apparatus Used in the Present Work.

Hardness Testing

One way to describe hardness is a material's ability to withstand localized plastic distortion, such as a tiny scratch or dent. Hardness and durability are frequently associated with one another in materials science. There are numerous kinds of tests for hardness. The most crucial are the penetration and indentation tests, which involve forcing a tiny indenter under controlled load and application rate conditions into the surface of a material to be examined. A hardness number is derived from measuring the depth or size of the resulting indentation; the softer the material, the greater and deeper the depression and the lower the hardness index number [17].

In the current study, the hardness of an AISI 304 stainless steel sample was tested using a Rockwell instrument, as seen in Figure 8. The applied stress was and the samples were cut into cubes. The hardness of the sample surface was measured at three different points, and the average of the three results was computed.

Figures 8: Hardness Device Used in the Present Research.

Results and Discussion

Introduction

This study is concerned with stainless steel that is subjected to exceptional conditions in the oil and gas industry. In reality, because of its profound effects on safety, conservation, and economics, this issue is a critical one for industry.

Every industry needs safe environments for its entire equipment in order to prevent environmental hazards and product loss. These include technical plant practices like shutdown, low efficiency addition, and product off features [18].

Actually, research and studies in this field are rare, as one can't find any local-specific studies about any kind of crack to compare outcomes. On the other hand, achieving this study was a real challenge, as the experiments and tests occurred in three research centers in Libya and were controlled by temper. All the reasons mentioned shrink

local research in this area, threaten any attempt to develop studies and lead local industrial companies to cooperate with regional research centers.
A number of experiments on a stainless steel fracture 304 in the Millitah plant have been conducted for this study. Prior to delving into the analysis, it is advisable to review the experimental limitations, which are deemed comparable to the regional report [10]. The failure investigations were carried out on the degassing system at the thermal incinerator, a branch of the third zone (superheated steam). The condition of this zone is severe as it deals with high temperatures and pressure, as illustrated in Figure 1. This zone is used to heat up high-pressure steam, which is considered saturated by the sensible heat of flue gas [19]. The fracture was situated beneath and roughly 10 centimeters from the valve. The following tests must be used in the required procedure: X-ray testing, chemical analysis, optical and micro fractography, measures of microhardness, and visual assessment.

Visual Inspection Results and Discussion
The AISI 304 stainless steel pipeline's cracks on one side are depicted in Figure 2.2. There were two cracks visible: one was parallel to the cross section, and the other was a lit above in a line that was horizontal. It is evident that three of the fissures were oriented horizontally. However, after cutting and releasing the sample shown in Figures 9a, b and c, it was discovered that the inside surface was entirely coated in dark gray sediments. Furthermore, it is evident that there are longitudinal cracks with some peripheral branching. Additionally, it has been seen that there is a shallow depression visible and that the surface surrounding the fissures is strained.
Actually, research and studies in this field are rare, as one can't find any local-specific studies about any kind of crack to compare outcomes. On the other hand, achieving this study was a real challenge, as the experiments and tests occurred in three research centers in Libya and were controlled by temper. All the reasons mentioned shrink local research in this area, threaten any attempt to develop studies, and lead local industrial companies to cooperate with regional research centers.

Figure 9a, b and c: The External Shape of the Specimen and the Approximate Length of the Notch after Cutting.

The inner surface's close-up photos at 1/100 magnification are displayed in Figures 10a, b and c, which also highlight the surface's dark gray tone and the magnitude of the fissure.

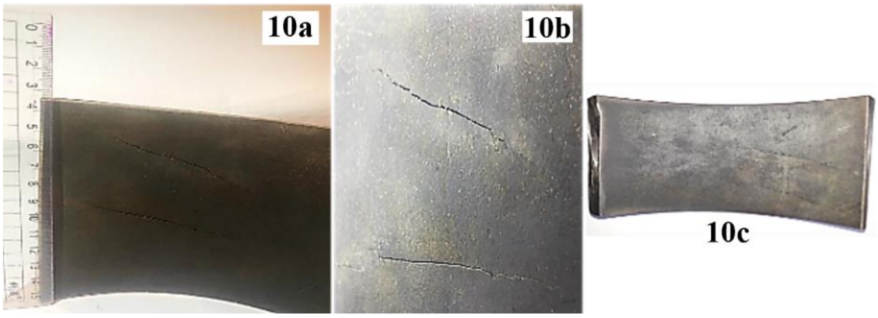

Figure 10a and b: Magnified Portion of the Crack from the Inner Surface and **Figure 10c:** The inner Surface of the Sample Covered with a Dark gray Sediment.

The crack is below the side, not away from the injection valve, as shown in Figure 2.2. It is best defined as a sectional parallel crack with no welding spots and a region that looks to be in good condition. In Figures 9 a, b, and c and 10 a, b, and c, the cracks can be clearly noticed after cutting and grinding, their lengths being about a few centimeters.
Six photos in Figure 11 shows examples of the structures that are exposed. Based on an analysis of the images, it can be concluded that crack bifurcations and their branches to the grain margins are present in images 1 and 2. However, pitting erosion is shown in images 3, 5, and 6.

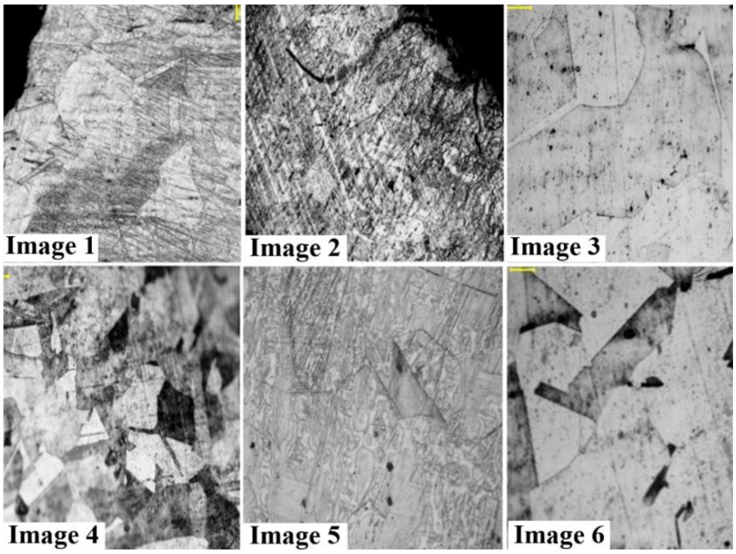

Figure 11: Microstructure of the Samples.

As can be seen in Figures 12a and b, comparing the reports of the Mellitah oil and gas complex, it was found that the failure happened due to the presence of tiny sub-cracks in the microscopic photographs of the same sample. On the surfaces of secondary fissures and cracks, there was additional sediment accumulation and covering. Also visible were the rivers on the fissures spanning the granules in Figure 12c.

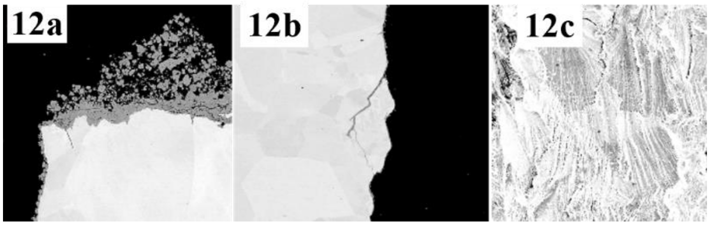

Figure 12a, b and c: SEM Images of AISI 304 Stainless Steel Pipe Cracks Belongs to Mellitah Oil and Gas Complex Report.

It can be noted that the fracture has crossed the grain boundaries based on the most recent figures. It can also report some deformation in the vicinity of the crack. It was also observed that there isn't another type of bulging.

X-Ray Fluorescence Analysis Results and Discussion

Table 1 showing the chemical composition of AISI 304 stainless steel weight percentage (wt.%).

Table 1: Chemical Composition of AISI 304 Stainless Steel.

Element	wt.%	Element	wt.%	Element	wt.%
Fe	71.1	Ni	7.79	Pb	<0.005
C	0.0226	Al	0.0014	Sn	0.096
Si	0.379	Co	0.243	B	<0.0001
Mn	1.58	Cu	0.203	Ca	<0.0001
P	0.0139	Nb	0.0111	N	0.101
S	0.0005	Ti	0.0037	Se	0.0199
Cr	18.2	V	0.105	Sb	0.0364
Mo	0.513	W	0.0080	Ta	0.0870
Fe	71.1	Ni	7.79	Pb	<0.005

As shown in Table 3.1, the element content in the stainless steel alloy AISI 304 was iron (Fe) with about 71.1 wt.%, followed by other important elements such as chromium (Cr), nickel (Ni), manganese (Mn), molybdenum (Mo), silicon (Si), cobalt (Co), and copper (Cu) with wt.% content of 18.2, 7.79, 1.58, 0.513, 0.379, 0.243, and 0.203, respectively. The other chemical element contents were less than 0.2 wt.%.

Hardness Testing Results and Discussion

Table 2 showing the hardness results, the obtained results for the chosen three locations were 77, 79 and 79 HRB, the average hardness of the three readings is 78.33 HRB. According to the ASM Aerospace International Specification Metals Inc. [20, 21], the hardness value of the stainless steel AISI 304 is 70 HRB, thus the obtained average hardness higher than of the international value with about 10.6%.

Table 2: Hardness Results for Stainless Steel AISI 304 Sample.

Location	Hardness Value (HRB)	Average (HRB)
1	77	78.33
2	79	
3	79	

Radiographic Testing Results and Discussion

Figures 13a and b show the X-ray images of the radiographic test, it can be noticed that there are some microcracks.

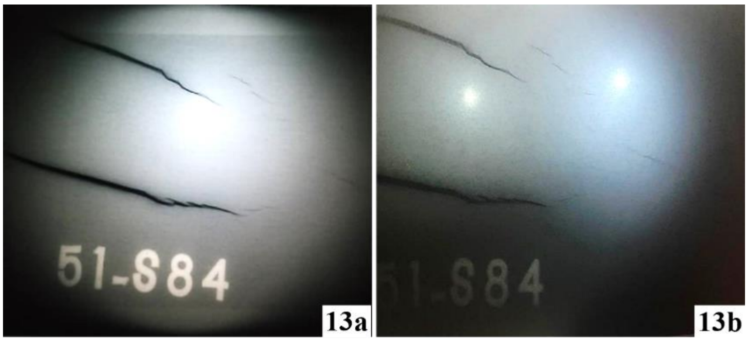

Figure 13: The X-Ray Radiographic Images.

Surface Investigations (Deposits and Structure)

Since high-pressure steam is the primary fluid in the AISA 304 Stainless Steel pipeline, this condition causes little spots to appear, as Figure 11 (images 3, 5, and somehow in image 6) clearly illustrates. These areas are known as pits, which lead to pitting failure. It is commonly recognized that this sort of corrosion can start other types of corrosion, such as uniform corrosion, stress corrosion, and fatigue corrosion. It can also go undetected and eventually penetrate the material. In actuality, greater temperatures throughout the production process can cause sensitization in austenitic stainless steels. The study specifically highlights the critical role that temperature-affected variations in oxide layer characteristics and their impact on pitting corrosion in AISI 304 stainless steel play [22].

In fact, this type of corrosion was present on the interior surface of the sample in this investigation without any indication of the methods used for measurement, such as depth, diameter, density of pits, or shapes. Furthermore, it was mentioned that one of the passivated metals that could suffer from pitting corrosion is stainless steel [22]. Nevertheless, scanning electron microscopy (SEM) images of Figures 12a and b (Millitah data) demonstrate how oxidation and grain boundary deterioration greatly affect the surface and cause the grains to break into fragments. Furthermore, the Millitah company report, which mentions the existence of deposits made up of iron (Fe), nickel (Ni), and chromium (Cr) oxides, was used to gather data for this study. in keeping with the inner pipeline's high steam pressure and temperature. One major element in failure is thought to be the formation of the aforementioned oxides [23].

Conclusion

The breakdown of a thermal incinerator in a binary fluid pipeline including deionized water and superheated steam was examined in this study. Austenitic stainless steel (AISI 304) is used to make the tube. After some time of operation under harsh circumstances with high temperatures (400 °C) and high pressures (46 bar), the failure is found. The injection valve is situated a few centimeters away from the failure. Depending on the results that were obtained, the following conclusions can be made:

I. The cracks had spread across cross-grain boundaries, and the breakdown started close to the valve;

II. Microstructure experiments showed that pitting corrosion exists;

III. The experiment results showed that certain sections of AISI 304 were under transgranular assault after the proper test was run.

IV. In the fracture region, there are deposits of Fe, Ni, and Cr that react with oxygen to form oxides;

V. Stress corrosion cracks (SCC) can be seen in AISI 304 at the elastic stress level, where the fractures resemble rivers.

Recommendations:

I. Mix points, for example, are advised to prevent corrosion and other damage processes. where operating limitations are being observed while using candela with various streams at various temperatures;

II. Spray nozzles, which are considered valuable devices, assist in dispersing the liquid into a spray. So, it can contribute to increasing the surface area of liquid, distributing liquid over a cross-sectional area, and working on witting the pipe wall apart from the injection point;

III. To encourage dispersion for immiscible streams, velocity should be maximized. Immiscible streams can persist as distinct phases inside the mixed stream, or for a new phase to emerge after the injection or process mix point;

IV. Refinery process streams may be supplemented with wetting agents to encourage the interaction of corrosion inhibitors and filming agents.

References

[1] Davis, Joseph R., ed., Stainless Steels. ASM Specialty Handbook. Materials Park, OH: ASM International. ISBN 978-0871705037, 2021. https://en.wikipedia.org/wiki/Stainless_steel.

[2] Sukanya Hägg Mameng, Localized Corrosion and Atmospheric Corrosion of Stainless Steels, KTH Royal Institute of Technology, School of Engineering Sciences in Chemistry, Biotechnology and Health, Department of Chemistry Division of Surface and Corrosion Science, SE-100 44 Stockholm Sweden, Doctoral Thesis, 2019. https://www.divaportal.org/smash/get/diva2:1369553/FULLTEXT01.pdf.

[3] TG 550's Proposed NACE New Standard, Corrosion inhibition management for oil and gas fields. Houston, TX: NACE International, 2019. https://www.researchgate.net/publication/43656192.

[4] Hughes, B., Total Systems Approach Handbook for Production Chemicals, 2e (eds. N. Atzmiller and R. Fisher). Baker Hughes Incorporated Liquid-dominated Systems (pp. 22–46) & Gas-dominated Systems (pp. 50–70), 2013. https://doi.org/10.1016/j.arabjc.2010.09.017.

[5] John Scott Pavelich, Corrosion of Aluminum Alloys in Wastewater Treatment Aeration Tanks, Department of Chemical and Materials Engineering University of Alberta, Master of Science, 2013. https://era.library.ualberta.ca/items/5e1d2260-52cb-4b10-b2de-82f1534ceaa9/view/a483e449-3165-4654-9f1a-d6fa415e270e/Pavelich_J_Scott_201703_MSc.pdf.

[6] Brahim El Ibrahimi and Lei Guo, Azole-Based Compounds as Corrosion Inhibitors for Metallic Materials, DOI: 10.5772/intechopen.93040, ISBN: 978-1-83968-180-6, 2020. https://www.intechopen.com/chapters/72699.

[7] Yahya T. Al-Janabi, An Overview of Corrosion in Oil and Gas Industry: Upstream, Midstream, and Downstream Sectors, Research and Development Center, Saudi Aramco, Dhahran, 31311, Saudi Arabia, Corrosion Inhibitors in the Oil and Gas Industry, First Edition, 2020. https://application.wileyvch.de/books/sample/352734618X_c01.pdf.

[8] A. Y. El-Etre, Inhibition of C-Steel Corrosion in Acidic Solution Using the Aqueous Extract of Zallouh Root, Department of Chemistry, Faculty of Science, Benha University, Benha 13518, Egypt, ScienceDirect, Materials Chemistry and Physics 108, 278–282, 2008. https://fsc.stafpu.bu.edu.eg/Chemistry/1547/publications/Ali%20Y%20El-Etre_zallouh.pdf.

[9] Viera Zatkalíková, et. al., Corrosion Behavior of Sensitized AISI 304 Stainless Steel in Acid Chloride Solution, Department of Materials Engineering, Faculty of Mechanical Engineering, University of Žilina, Univerzitná 8215/1, 010 26 Žilina, Slovakia, Materials, 158543, 2022. https://www.doi.org/10.3390/ma15238543.

[10] A. Arifin, et, al., Failure Analysis of AISI 304 Stainless Steel Pipeline Transmission a Petrochemical Plant, Department of Mechanical Engineering, Faculty of Engineering, Universitas Sriwijaya, Indralaya, 30662, Sumatera Selatan, Indonesia, IOP Conf. Series: Materials Science and Engineering 857 - 012006 DOI:10.1088/1757-899X/857/1/012006, 2020. https://repository.unsri.ac.id/99780/1.

[11] Wei-min Guo, et. al., Stress Corrosion Cracking of a 304 Stainless Steel Elbow, Qilu University of Technology (Shandong Academy of Sciences), China, Journal of Failure Analysis and Prevention 20(1), DOI: 10.1007/s11668-020-00852-7, 2020. https://www.researchgate.net/publication/339852095.

[12] Jamshed Alam, Nondestrucive Testing. Departmen of Mechanical Engineering, University of Mohammed Ali Jauhar, Rampur-244901 U. P. India, 2018. https://www.slideshare.net/slideshow/jamshed-alam-seinar-report-copy/120256692.

[13] J. Sanderson, Fundamentals of Microscopy. Current Protocols in Mouse Biology, 10, e76. DOI: 10.1002/cpmo.76, 2020. https://www.researchgate.net/publication/341918746.

[14] Yang Leng, Materials Characterization: Introduction to Microscopic and Spectroscopic Methods, Second Edition. Published by Wiley-VCH Verlag GmbH & Co. KGaA, 2013. https://application.wileyvch.de/books/sample/3527334637_c01.pdf.

[15] Hasna Ait Bouh, X-Ray fluorescence Technique Analysis (Principles and instrumentations), National Center for Energy Sciences and Nuclear Techniques, Morocco, Publisher: Muruz, ISBN: 978-620-2-78771-0, 2020. https://www.researchgate.net/publication/371256230.

[16] Deyab M. A., Adsorption and Inhibition Effect of Ascorbyl Palmitate on Corrosion of Carbon Steel in Ethanol Blended Gasoline Containing Water as a Contaminant, Corrosion Science, Volume 53, Issue 8, Pages 2592-2597, 2024. https://www.sciencedirect.com/science/article/abs/pii/S0010938X11002071.

[17] Layla M. Hasan, Hardness Test, Mustansiriyah University, College of Engineering, Baghdad, Iraq, Lecture Notes: (Lecture 6), 2021. https://uomustansiriyah.edu.iq/media/lectures/5/5_2020_03_19!06_35_43_PM.pdf.

[18] Samuel A. Bradford, Corrosion Control, Metallurgical Engineering University of Alberta, T5H 3J7, Canada, ISBN: 1-894038-58-4, 2001. http://www.casti.ca.

[19] ASM Aero Spacing Specification Metals Inc., AISI Type 304 Stainless Steel, 800 398-4345, Metals Handbook, 10th ed., vol. 1, ASM International Handbook Committee., ASM International, Materials Park, OH, 1990. https://asm.matweb.com/search/SpecificMaterial.asp?bassnum=mq304a.

[20] Xianjun Lei, et. al., Self-Induced Internal Corrosion Stress Transgranular Cracking in Gradient-Structural Ploycrystalline Materials at High Temperature, Department of Materials Science and Engineering, Harbin Institute of Technology, Harbin 150001, China, Journal Metals, 11(9), 1465; https://doi.org/10.3390/met11091465, 2021. https://www.mdpi.com/2075-4701/11/9/1465.

[21] Sanni O., et. al., Evaluation of Corrosion Inhibition of Essential Oil-Based Inhibitors on Aluminum Alloys, Department of Chemical Engineering, Faculty of Engineering, Built Environment and Information Technology, University of Pretoria, Pretoria 0028, South Africa, ACS Omega, 7 (45), 40740−40749, 2022. https://www.researchgate.net/publication/365137067.

[22] Francisco-Javier Cárcel-Carrasco, et. al., Pitting Corrosion in AISI 304 Rolled Stainless Steel Welding at Different Deformation Levels, ITM, Polytechnic University of Valencia, 46022 Valencia, Spain, Journal of Appl. Sci., 9, 3265; DOI:10.3390/app9163265, 2019. www.mdpi.com/journal/applsci.

[23] Ashit Kumar Pramanick, et. al., Failure Investigation of Super Heater Tubes of Coal Fired Power PlantMaterials Science & Technology, CSIR – National Metallurgical Laboratory, Jamshedpur 831007, India, Volume 9, Pages 17-26, 2017https://doi.org/10.1016/j.csefa.2017.06.001, https://www.researchgate.net/publication/317495619.